4th Conference on Production Systems and Logistics

Synthesis of Artificial Coating Images and Parameter Data Sets in Electrode Manufacturing

Achim Kampker[1], Heiner Heimes[1], Benjamin Dorn[1],
Henning Clever[1], Marcel Drescher[1], Robert Ludwigs[1]
[1]*Production Engineering of E-Mobility Components (PEM), RWTH Aachen University, Aachen, Germany*

Abstract

Driven by continuous cost pressure and increasing market requirements, the optimization of lithium-ion battery production is the focus of attention. To save time and costs, machine learning represents a promising tool. But a considerable amount of training data is needed. Since data is not always available to the required extent, approaches for synthesizing artificial data were investigated. In this study, the quality and corresponding measurement parameters in electrode production were assessed and selected. Based on this selection, coating trials have been conducted and the corresponding data set collected. The data set forms the basis for the synthesis of artificial coating images and parameters. The selection and design of the synthesis models were divided into two sub-steps. First, the synthesis of artificial coating images was investigated. A promising method for the data synthesis of (coating) images is Generative Adversarial Networks (GAN). The basic idea of GANs is to oppose two models: a discriminator and a generator. The generator generates artificial data samples that match the input of the training data set. Afterward, those data samples (both input and artificial data) are introduced to the discriminator. The discriminator's function is to identify whether the data presented originates from the training data set or whether it is a counterfeit (artificial data) of the generator. In a second step, the synthesis of new parameter sets in the form of tabular data is investigated. The requirements for the synthesis of tabular data sets correspond in principle to those for multivariate regression analysis. The combination of the models resulted in a method that allows the prediction of the corresponding measured quality values for arbitrarily selected process parameters, as well as the visualization of the associated coating result in the form of an artificial image.

Keywords: Machine Learning; Generative Adversarial Networks; Data Synthesis; Electrode Manufacturing

1. Introduction

Due to their various properties, lithium-ion batteries have come to the fore as an energy source for mobile applications. As demand increases, so do the demands on their quality, performance, and service life, coupled with steadily growing cost pressure. To meet these requirements, not only further technological development and research in the field of cell technology is needed, but also continuous optimization of the production processes. In this context, the production of electrodes in particular represents a complex sub-step in cell manufacturing. [1] It has a large number of adjustable production parameters with complex influences on the quality characteristics of the electrodes. [2,3] This complexity makes it difficult to analyze the interrelationships and thus to find suitable parameter combinations for the desired production results.

Data-driven approaches are becoming increasingly important for such use cases. For example, image recognition processes trained by means of artificial intelligence can be used to detect production defects and thus

DOI: https://doi.org/10.15488/13485
ISSN: 2701-6277

help in the automated optimization and control of production processes. [4] Just as the development of human intelligence requires a large number of experiences and perceptions over the course of a lifetime, machine learning algorithms must generally be confronted with many observations in order to make accurate predictions. For this reason, machine learning algorithms usually require large amounts of data for their training. In many areas, however, these are not available in the required amount and can only be obtained with difficulty, for example at enormous expense in terms of time and money. [5] In the production of electrodes for lithium-ion cells, for example, the large number of production parameters and their complex interrelationships regarding the production result makes it very difficult to collect large amounts of data for process optimization supported by machine learning methods. Synthetically generated data sets represent an economically interesting alternative to obtaining real test data.

For this reason, an approach to synthesizing artificial electrode coating test data was investigated. Both structured (tabular) and unstructured data (image data) were artificially generated. As a data basis, a reference data set was first created experimentally. For this purpose, tests were carried out on a pilot production line and corresponding quality parameters were measured. The basics of electrode production as well as the models and machine learning algorithms used are introduced in chapter 2. The experimental setup and data preparation, as well as the design of the models for data generation, are described in chapter 3. An overview of the achieved results is given in chapter 4, while chapter 5 summarizes the main conclusions. This study demonstrates that synthetic coating images and their associated process data can be generated using artificial intelligence. However, it is necessary to conduct further research to assess the suitability of this approach as a standalone data source, rather than relying on real data.

2. Fundamentals

In the following chapter, the technical principles of electrode manufacturing and relevance of surface inspection as well as the fundamentals of applying GANs and regression using multilayer perceptron networks (MLP) are established.

2.1 Electrode manufacturing for lithium-ion batteries

Figure 1 shows an overview of the manufacturing processes of electrode manufacturing for lithium-ion battery cells. First, the active material for the electrodes is mixed from several powder components and the solvent to produce the so-called slurry. In the coating step, the slurry is coated onto a metal foil as a thin film and dried afterwards. During calendering, the film is compressed by applying a line load over a roller arrangement to reduce the porosity of the coated material. The electrodes are then cut or punched into the desired shape. This marks the end of electrode manufacturing, which is followed by cell assembly. [6] The work of this paper is focused in particular on the front-end processes from weigh-in of materials, over mixing, to coating and drying.

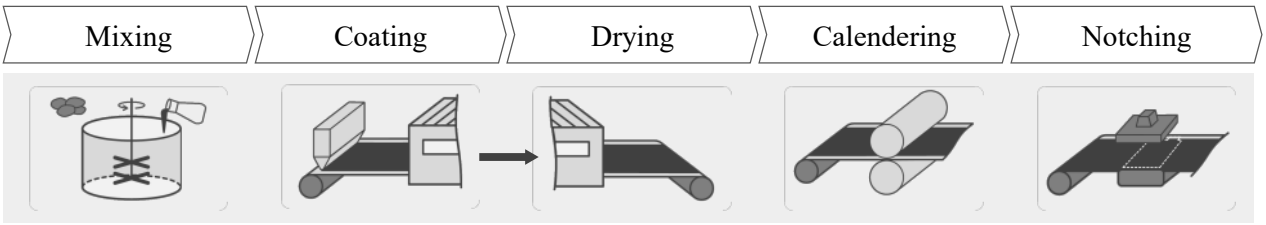

Figure 1: Schematic view of the steps in electrode production [4]

Surface inspection during electrode manufacturing is critical for process control and minimizing scrap rates. By carefully examining the surface of the electrodes, manufacturers can identify and address any defects or irregularities that may affect the performance of the final product. This helps to ensure that the electrodes meet the required specifications and are of high quality. In addition, surface inspection can help identify

potential issues early in the manufacturing process, allowing manufacturers to take corrective action (e.g. based on machine learning algorithms) and prevent defective electrodes from being produced. This ultimately leads to lower scrap rates, as fewer defective electrodes need to be discarded, and helps to reduce costs and improve overall efficiency in the manufacturing process. Optical imaging of electrode coatings thereby presents a consistent and automatable solution for the detection of defects. [7]

Choudhary et al. present a promising approach to detect and classify mechanical defects in real time [4]. Also, in other research areas, especially in the medical field, image analysis by means of artificial intelligence have been widely explored in recent years. [8,9] Since the problem of lack of data also exists in the medical setting, Kanayama et al. developed a GAN-based model for the synthesis of endoscopic images for gastric cancer detection [10]. Also, Sedigh et al. used a GAN to generate synthetic skin cancer images to compensate for insufficient data for training a proposed CNN algorithm. [11] Generally, GANs are capable of generating very realistic high-resolution images [12], which make them a viable solution for the presented use case. However, no work could yet be found on image generation in the context of electrode coating. The experimental setup and data basis will be explained in chapter 3.

2.2 Generating synthetic images using generative adversarial networks

The basic idea of GANs is to introduce two opposing models: A discriminative model and a generative model. The generator receives random noise (training data) as input and generates data samples (matching the form of the training data), that are later presented to the discriminator. The task of the discriminator is to identify whether the given sample originated from the training dataset or whether it is a "fake" of the generative model. Mutual competition drives both models to keep improving their methods until the counterfeits are so similar to the originals, that it is no longer possible to distinguish them. Both the generator and the discriminator are typically constructed as deep neural networks and use the binary cross entropy for optimization. [13] When a GAN-trained generator is used to synthesize data, the output cannot be precisely controlled. For example, if the training data set includes data that can be categorized, the classic GAN method cannot be used to specify which category the generated data should come from. Depending on the application, it may be necessary to control the output of the generator. In this case, conditional generative adversarial networks (CGAN) as shown in Figure 2 represent an alternative.

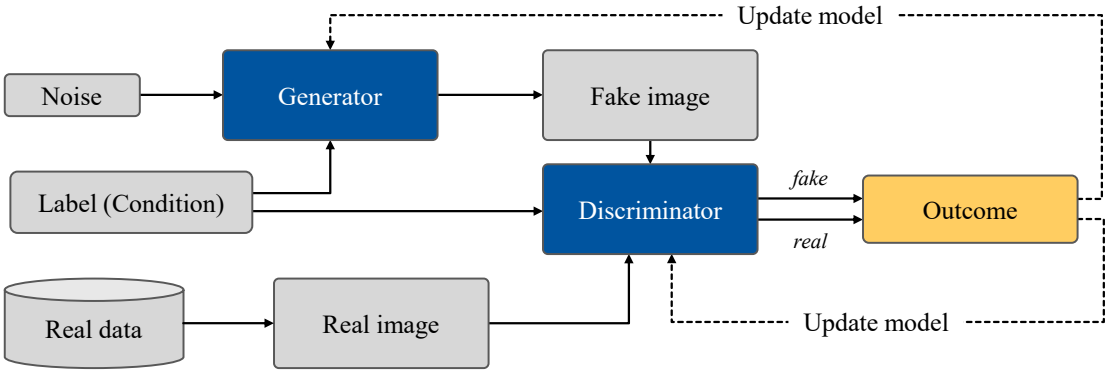

Figure 2: Schematic structure of a Conditional Generative Adversarial Networks (CGAN) [14]

In this case, in addition to the latent vector, a label expressing the membership to a class is passed to the generator and discriminator. The training data set, which is used to train the model must also be labelled. The information of the label is linked with the random signal noise and thus serves as input signal for the data synthesis. In addition to the data point to be evaluated, the discriminator is also provided with the label, which is linked with the input data point (image). [15]

2.3 Regression using multilayer perceptron networks

MLPs are a type of feedforward neural network, that can be used as universal approximators and represent any continuous function. As the name suggests, an MLP is composed of several layers. Between the input layer and the output layer, there is any number of hidden layers. The number of neurons in the input layer is equal to the number of input values. Since in this work three parameters are varied, this also corresponds to the number of input neurons. Analogously the number of neurons in the output layer corresponds to the number of output values. The definition of the number of hidden layers and neurons in each hidden layer are hyperparameters that can be tuned during the optimization process. [5]

3. Methods

The following chapter introduces the experimental design used to generate the data basis as well as the data preprocessing and model design for data synthesis of electrode coating images.

3.1 Experimental design and data acquisition

In order to investigate the coating process, electrodes with different process parameters are produced. For this purpose, three sets of trials are conducted using graphite slurries with different material ratios for the production of anodes. Regarding the processability of the slurry, its viscosity plays a major role. [16] For this reason, the proportion of carboxymethyl cellulose binder (CMC), which significantly controls the viscosity properties, is slightly varied for each test series. Table 1 shows the formulations of the test series for three different slurries. Starting from the basic formulation (Slurry 1), which is based on industrial experience [17], the mass fraction of the CMC binder is slightly increased and reduced. The mass ratios of the other components remain the same relative to each other, resulting in their quantities.

Table 1: Slurry formulations for graphite anodes

Material	Slurry 1	Slurry 2	Slurry 3
Graphite (SG3)	564,00 g	562,30 g	565,70 g
CMC binder	12,00 g	16,00 g	8,00 g
Carbon black	6,00 g	5,98 g	6,02 g
SBR binder	45,00 g	44,87 g	45,14 g
Dist. Water	706,00 g	703,85 g	708,14 g

The electrodes are coated in a roll-to-roll coating line with a slot die for single-sided coating and two drying units. The adjustable parameters of the system are the distance between the slot die and the metal film (which is kept constant at 200 µm), the web speed, and the speed of the feed pump. Table 2 shows the abbreviated representation with the indication of the respective value ranges. To be able to map the influences of the individual parameters, a full factorial experimental design is conducted.

Table 2: Varied test parameters during the full factorial coating trials

Parameter	Value settings
Formulation	Slurry 1; Slurry 2; Slurry 3
Web speed	0.5 m/min; 1.0 m/min; 1.5 m/min
Pump speed	100 rpm; 125 rpm; 150 rpm; 200 rpm

Figure 3 shows extracts of the recorded coating images showing different coating patterns. It is striking that in many cases there is no continuous film. Rather, the coating patterns show defects or line or grid patterns. Also, drying flaws can be observed at high pump speeds and low web speeds. In addition to the images, quality characteristics such as wet film thickness and viscosity of the slurries are recorded. The coating images reveal a strong correlation to the wet film thickness. The ideal wet film thickness is in the range of

120 µm to approx. 200 µm for the defined drying parameters from a process engineering point of view, at which neither coating nor drying defects occur.

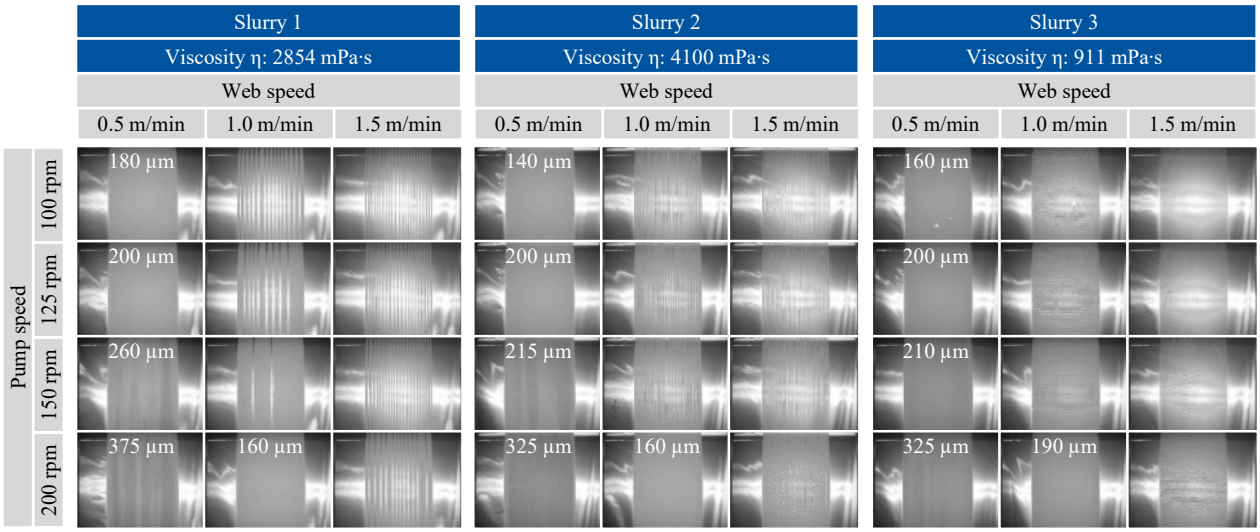

Figure 3: Extract of characteristic images of electrode coatings from the experimental test series

3.2 Data preparation and pre-processing

As previously described, about half of the coating runs do not show a continuous coating film. Rather, line or grid patterns appear. Since in this case there is no wet film thickness to be measured for the respective coatings, a new parameter is introduced to evaluate the test results. The aim is to show what percentage of the film is coated (coating area). For this purpose, the coating images are imported and processed in Python with the help of the scikit-image software library. By applying a grayscale filter, each pixel of the image is assigned a value between 0 and 255 depending on the brightness of the pixel. The values are stored in a matrix with the resolution of the original images (2448x2046).

In the next step, the images are cropped to the coating area, removing the remaining film areas on both sides that do not contain coating. Afterward, a threshold is set for the pixel values above which all values are raised to 255 (white) and set to 0 (black) below. The result is a binary image consisting only of black and white pixels. Dynamic adjustment of the threshold value ensures that, regardless of the exposure of the image, the coated areas appear black and the uncoated areas appear white. Based on the binary image, the proportion of black pixels and thus the proportion of coated area can be calculated for each coating image.

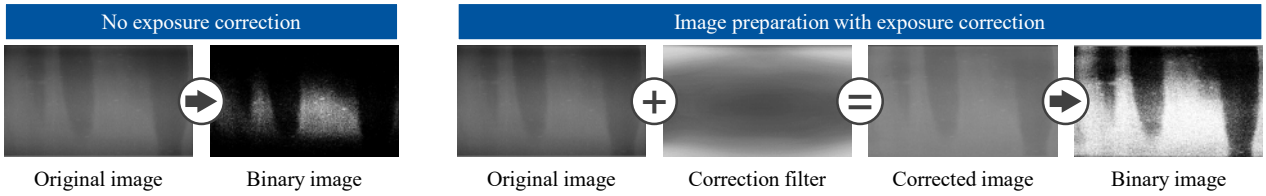

Figure 4: Conversion of the input coating images to binary images including exposure correction

The same principle is used to analyze the images of the coatings that have not fully dried. Since the pixel values (gray levels) of the dry and wet areas are closer together, the determination of the limit value must be much more precise. Another complicating factor is that the images are not evenly illuminated by the camera's flash. Pixel values assigned to the dry state in one image area might describe moist zones in other image areas. In order to compensate for this effect, a brightness filter, as shown in Figure 4, is applied over all images. Since the relative illumination by the flash is almost identical on all images and only the absolute brightness values differ (presumably due to ISO adjustment of the camera), the filter is created manually

based on a few images and does not require any dynamic adjustment. Figure 4 shows an example of the binary distribution with and without the filter.

By additionally determining the coating and drying area, a label is assigned to each image. If the edge at the start or end of a coating or bare copper foil is visible on the image, the label *foil edge* is assigned. All other labels are assigned depending on the fraction of coated or dried area. Coating images with a line or grid pattern are considered partly coated and receive values as *coated40*, [...], *coated100*, which indicate the percentage of coated (in increments of ten). The label *coated50* for example describes a coating image, with which the fraction of the coated area accounts for 50-59 %. Complete coatings are labeled as *coated100*. Furthermore, fully coated but not fully dried images are labelled likewise as *dried20*, *dried30*, [...], *dried90*. If the image showed a flawless, fully dried, and continuous coating, the label *OK* was assigned.

To reduce the demand for data storage the image areas of lesser interest (uncoated edges) were cropped and the images were scaled down from their original format of 2448x2046 pixels to 205x128. Furthermore, the pixel values of the images were normalized between -1 and +1 using *MinMax*-normalization.

3.3 Design of the Conditional Generative Adversarial Network

Since the aim of this paper is to generate data points representing different coating patterns according to the labeling logic mentioned above, a CGAN was chosen for image generation. The generator and discriminator were designed as fully interconnected neural networks. The dimension of the latent vector was set to 100. Its values are random but constrained between 0 and 1. The first level of the generator, therefore, comprised 100 neurons. Since the scaled coating images have a resolution of 205x128 pixels, the input level of the discriminator has 26,240 neurons. This also corresponds to the number of neurons in the output layer of the generator. The labels were numbered and embedded into the input layers of each model. As the discriminator returns only one value, it also has only one neuron in the output layer. The models are trained in 50,000 epochs with a batch size of 128. The Adam algorithm [18] is chosen as the optimizer with a learning rate of 0.0002 and a momentum of 0.5.

3.4 Regression of coating parameters

The first modeling approach investigated uses linear regression. The assumption was made that the relationships between the dependent and independent variables are linear. This assumption represents a simplification that can be justified on the basis of the course of the measured data.

The second modeling approach investigated is realized by the construction of an MLP network that contained two hidden layers with 64 neurons each. Rectified linear unit functions (ReLU) are chosen as activations with the exemption of the output layer for the parameters that represent the fractions of coated and dried areas, as they are limited between 0 and 1. Therefore a sigmoid function was used. The chosen error function is the mean squared error and optimization uses the Adam algorithm with a learning rate of 0.001.

4. Results

In this chapter, the results from the synthesis of the coating images are discussed and the application of a combined model to synthesize tabular data sets is validated.

4.1 Synthesis of the coating images

As can be seen in Figure 5, the developed CGAN is capable of generating coating images that are very realistic to human perception, representing all types of defects that occur in the training data set. For some predefined categories, the generated images show great similarity to the corresponding real images (e.g. *coated70*). This can be attributed to little variation in the images of the affected categories of the training dataset. In addition, the generated images show minor distortions in the form of noise.

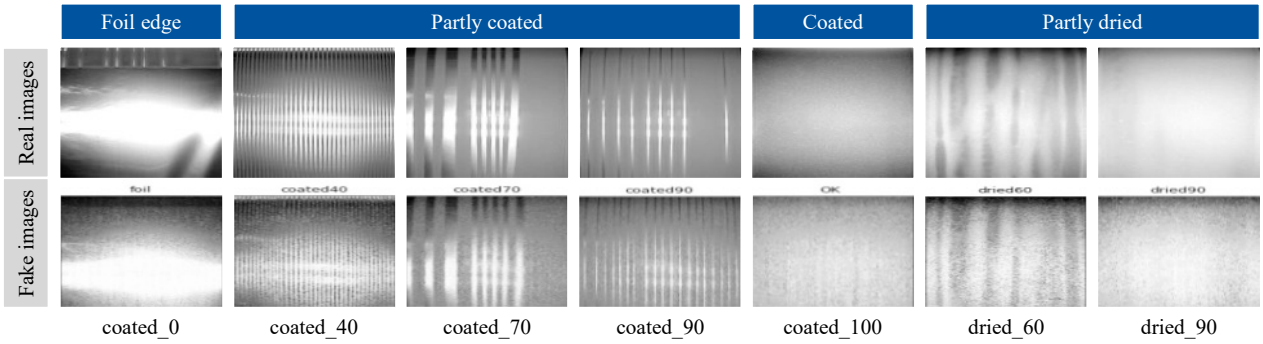

Figure 5: Coating images generated by CGAN

The validation of the "computational" quality of synthetic images remains a focus of current research. The most commonly used quantitative metric for evaluating artificially generated images is the *Fréchet Inception Distance* (FID). [19] The goal of this is not to analyze the generator or discriminator, but rather to take a more outcome-based approach in which generated images are compared to real images and a similarity score between them is determined. [20] The score is calculated by using the *Inception-v3* model. [21] Table 3 shows the results for comparisons of randomly selected batches of 500 images each.

Table 3: FID-Scores for batches of 500 images

Compared batches	Real-1, Real-1	Real-1, Real-2	Real-1, Artificial
FID score	0	70	220

As expected, the FID score for the comparison of two identical batches is 0. The FID score of two batches of real images represents the reference score to aim for. The comparison of real and artificial images shows FID scores about three times higher value than the desired reference score. [19]

4.2 Synthesis of tabular data set

For the synthesis of the tabular process parameter data sets, a simple linear regression model and a more generalizable MLP regression model were applied and evaluated. Figure 6 shows the results of the linear regression (top) and MLP regression analysis (bottom) for the dependent variable wet film thickness. For this parameter, the linear model shows a better fit toward the measured data. The error was quantified using the mean squared error, which reached values of 29.23 for the MLP model and 15.09 for the linear model.

The results for the regression of the fraction of coated area can be seen in Figure 7. Here the MLP regression (bottom) shows a slightly better fit toward the measured data, than the linear model (top). In this case in particular, it is evident that the linear regression produces counterintuitive results (i.e. fraction of coated area greater than 100 %). This prediction requirement is addressed by the MLP. The mean squared error for the MLP model was calculated at 0.10, whereas the error for the linear model is 0.13. In order to achieve the best possible results and generate a fully synthesized dataset, the constructed models of the CGAN and MLP were combined. The structure of the combined models is shown in Figure 8.

For the approximation of the wet film thickness the linear model is used and the fractions of coated and dried areas are calculated by the MLP regression, since these models show the smallest errors as shown in Figure 6 and Figure 7. The values for the fraction of coated and dried areas represent the type and severity of the examined error and thus are transformed into the label that serves as input for image generation.

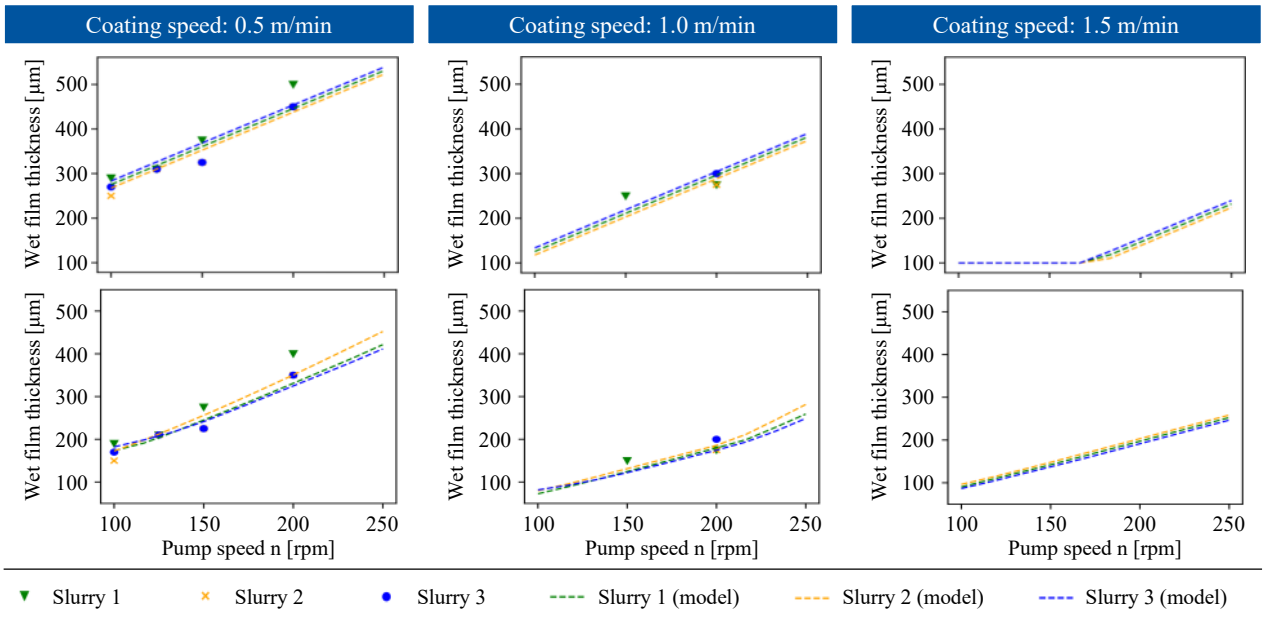

Figure 6: Prediction of the wet film thickness using linear regression (top) and MLP-regression (bottom)

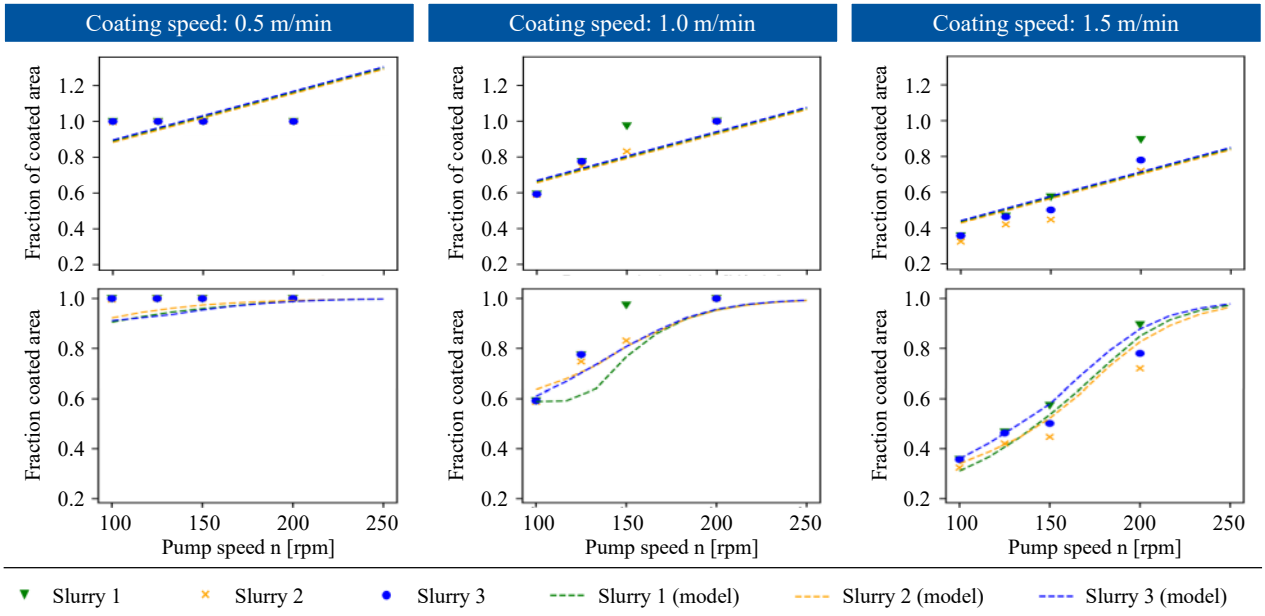

Figure 7: Prediction of the fraction of coated area using linear regression (top) and MLP-regression (bottom)

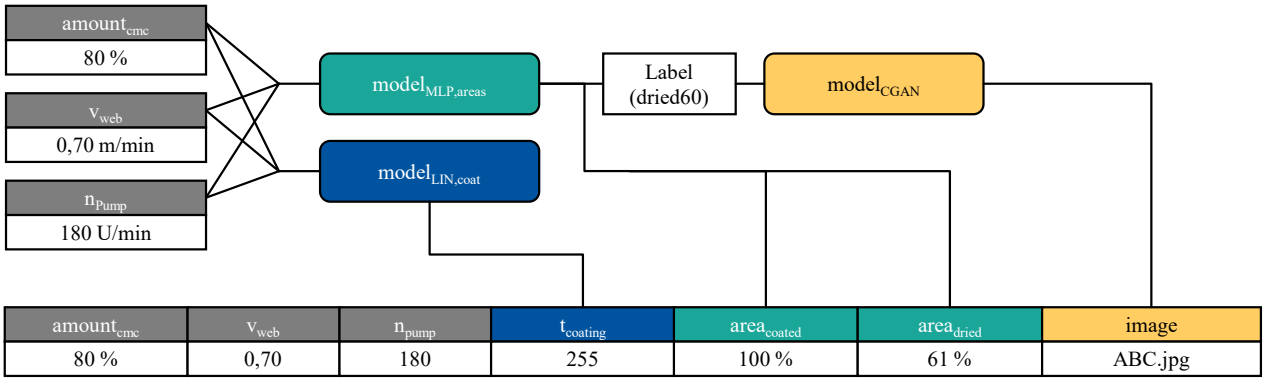

Figure 8: Structure of the combined overall model for data synthesis of electrode coating images

5. Conclusion

The production of electrodes for lithium-ion cells represents a complex manufacturing process with strong influences on the quality of the battery cells. To save time and costs, machine learning methods can provide helpful support for ensuring the quality of the coating process. They are capable of analysing and evaluating complex correlations and abstract data spaces, for which, however, they require a great amount of training data. To provide this amount of input even with limited availability of real test data, an approach to synthesizing artificial coating data by using a CGAN was proposed. The results show that the combination of a linear regression model and an MLP regression model for synthesizing structured data together with a CGAN for synthesizing coating images is capable of generating an artificial data set. The computational quality of the artificial data was evaluated using the Fréchet Inception Distance and could be sufficiently confirmed. However, the commonly applied evaluation metrics are still part of current research. When viewed with the human eye, the quality of the generated images can be considered good. Only a pixel-like noise is visible on many artificially generated images. In summary, this study shows that synthetic coating images and the associated process data can be generated using artificial intelligence. However, further research is needed to evaluate the viability of the artificially generated images and datasets as a stand-alone data source, rather than relying on real data.

Acknowledgements

This work is based on research results within the project “DataBatt”. The project has received funding from the German Federal Ministry of Education and Research (BMBF) under the funding code 03XP0323A. The authors are responsible for the content of this publication.

References

[1] Hawley, W.B., Li, J., 2019. Electrode manufacturing for lithium-ion batteries—Analysis of current and next generation processing. Journal of Energy Storage 25, 100862.

[2] Mohanty, D., Hockaday, E., Li, J., Hensley, D.K., Daniel, C., Wood, D.L., 2016. Effect of electrode manufacturing defects on electrochemical performance of lithium-ion batteries: Cognizance of the battery failure sources. Journal of Power Sources 312, 70–79.

[3] Smekens, J., Gopalakrishnan, R., Steen, N., Omar, N., Hegazy, O., Hubin, A., van Mierlo, J., 2016. Influence of Electrode Density on the Performance of Li-Ion Batteries: Experimental and Simulation Results. Energies 9 (2)

[4] Choudhary, N., Clever, H., Ludwigs, R., Rath, M., Gannouni, A., Schmetz, A., Hülsmann, T., Sawodny, J., Fischer, L., Kampker, A., Fleischer, J., Stein, H.S., 2022. Autonomous Visual Detection of Defects from Battery Electrode Manufacturing. Advanced Intelligent Systems 6, 2200142.

[5] Hagan, M.T., Demuth, H.B., Beale, M.H., Jesus, O. de, 2014. Neural network design, 2nd edition ed. Amazon Fulfillment Poland Sp. z o.o, Wrocław, Amazon, Wrocław, 800 pp.

[6] Heimes, H.H., Kampker, A., Lienemann, C., Locke, M., Offermanns, C., Michaelis, S., Rahimzei, E., 2018. Produktionsprozess einer Lithium-Ionen-Batteriezelle, 3. Auflage, [revidierte Ausgabe] ed. PEM der RWTH Aachen; VDMA, Aachen, Frankfurt am Main, circa 24 ungezählte Seiten.

[7] Reynolds, C.D., Slater, P.R., Hare, S.D., Simmons, M.J.H., Kendrick, E., 2021. A review of metrology in lithium-ion electrode coating processes. Materials & Design 209, 109971.

[8] Hirasawa, T., Aoyama, K., Tanimoto, T., Ishihara, S., Shichijo, S., Ozawa, T., Ohnishi, T., Fujishiro, M., Matsuo, K., Fujisaki, J., Tada, T., 2018. Application of artificial intelligence using a convolutional neural network for detecting gastric cancer in endoscopic images. Gastric cancer : official journal of the International Gastric Cancer Association and the Japanese Gastric Cancer Association 21 (4), 653–660.

[9] Liu, W., Anguelov, D., Erhan, D., Szegedy, C., Reed, S., Fu, C.-Y., Berg, A.C., 2016. SSD: Single Shot MultiBox Detector, in: Leibe, B., Matas, J., Sebe, N., Welling, M. (Eds.), Computer Vision – ECCV 2016, vol. 9905. Springer International Publishing, Cham, pp. 21–37.

[10] Kanayama, T., Kurose, Y., Tanaka, K., Aida, K., Satoh, S.'i., Kitsuregawa, M., Harada, T., 2019. Gastric Cancer Detection from Endoscopic Images Using Synthesis by GAN, in: Shen, D., Liu, T., Peters, T.M., Staib, L.H., Essert, C., Zhou, S., Yap, P.-T., Khan, A. (Eds.), Medical Image Computing and Computer Assisted Intervention – MICCAI 2019, vol. 11768. Springer International Publishing, Cham, pp. 530–538.

[11] Sedigh, P., Sadeghian, R., Masouleh, M.T., 2019 - 2019. Generating Synthetic Medical Images by Using GAN to Improve CNN Performance in Skin Cancer Classification, in: 2019 7th International Conference on Robotics and Mechatronics (ICRoM). 2019 7th International Conference on Robotics and Mechatronics (ICRoM), Tehran, Iran. 20.11.2019 - 21.11.2019. IEEE, pp. 497–502.

[12] Zhang, B., Gu, S., Zhang, B., Bao, J., Chen, D., Wen, F., Wang, Y., Guo, B., 2021. StyleSwin: Transformer-based GAN for High-resolution Image Generation.

[13] Goodfellow, I.J., Pouget-Abadie, J., Mirza, M., Xu, B., Warde-Farley, D., Ozair, S., Courville, A., Bengio, Y., 2014. Generative Adversarial Networks.

[14] MathWorks Inc. Train Generative Adversarial Network (GAN). https://de.mathworks.com/help/deeplearning/ug/train-generative-adversarial-network.html. Accessed 30 October 2022.

[15] Mirza, M., Osindero, S., 2014. Conditional Generative Adversarial Nets.

[16] Schmitt, M., Baunach, M., Wengeler, L., Peters, K., Junges, P., Scharfer, P., Schabel, W., 2013. Slot-die processing of lithium-ion battery electrodes—Coating window characterization. Chemical Engineering and Processing: Process Intensification 68 (4–5), 32–37.

[17] Wentker, M., Greenwood, M., Leker, J., 2019. A Bottom-Up Approach to Lithium-Ion Battery Cost Modeling with a Focus on Cathode Active Materials. Energies 12 (3), 504.

[18] Kingma, D.P., Ba, J., 2014. Adam: A Method for Stochastic Optimization.

[19] Borji, A., 2022. Pros and cons of GAN evaluation measures: New developments. Computer Vision and Image Understanding 215 (4), 103329.

[20] Heusel, M., Ramsauer, H., Unterthiner, T., Nessler, B., Hochreiter, S., 2017. GANs Trained by a Two Time-Scale Update Rule Converge to a Local Nash Equilibrium.

[21] Szegedy, C., Vanhoucke, V., Ioffe, S., Shlens, J., Wojna, Z., 2015. Rethinking the Inception Architecture for Computer Vision.

Biography

Henning Clever (*1992) is research associate at the Chair of Production Engineering of E-Mobility Components (PEM) at the RWTH Aachen University since 2019 and group lead for the research group Battery Production Management since 2021. He studied mechanical engineering specializing in production engineering at the RWTH Aachen University.

Marcel Drescher (*1994) is research associate at the Chair of Production Engineering of E-Mobility Components (PEM) at the RWTH Aachen University since 2022. He studied mechanical engineering at the RWTH Aachen University with a focus on automotive engineering.

Robert Ludwigs (*1993) is research assistant at the Chair of Production Engineering of E-Mobility Components (PEM) at RWTH Aachen University. He studied mechanical engineering with a specialization in production technology at RWTH Aachen University.

Benjamin Dorn (*1990) is research associate at the Chair of Production Engineering of E-Mobility Components (PEM) at the RWTH Aachen University since 2018 and chief engineer for Production Technology & Organization since 2021. He studied business administration and engineering specializing in mechanical engineering at the RWTH Aachen University.

Dr.-Ing. Heiner Hans Heimes (*1983) is executive chief engineer of the Chair of Production Engineering of E-Mobility Components (PEM) at the RWTH Aachen University since 2019. He studied mechanical engineering with a focus on production engineering at RWTH Aachen University. From 2015 to 2019, he was head of the Electromobility Laboratory (eLab) of RWTH Aachen University.

Prof. Dr.-Ing. Achim Kampker (*1976) is head of the chair "Production Engineering of E-Mobility Components" (PEM) of RWTH Aachen University. Prof. Dr. Kampker also acts as member of the executive board of the "Fraunhofer Research Institution for Battery Cell Production FFB" in Münster. He is involved in various expert groups of the federal and state governments.